OPEN ACCESS

Original research

Visibility of liquid embolic agents in fluoroscopy: a systematic in vitro study

Niclas Schmitt ,[1] Lena Wucherpfennig ,[2] Sophia Hohenstatt ,[1] Charlotte S Weyland ,[1] Christof M Sommer,[3,4] Martin Bendszus,[1] Markus A Möhlenbruch,[1] Dominik F Vollherbst [1]

► Additional supplemental material is published online only. To view, please visit the journal online (http://dx.doi.org/10.1136/neurintsurg-2022-018958).

[1]Department of Neuroradiology, University Hospital Heidelberg, Heidelberg, Germany
[2]Department of Diagnostic and Interventional Radiology, University Hospital Heidelberg, Heidelberg, Germany
[3]Clinic of Radiology, University Hospital Heidelberg, Heidelberg, Germany
[4]Clinic of Radiology and Neuroradiology, Sana Kliniken Duisburg GmbH, Duisburg, Germany

Correspondence to
Dr Dominik F Vollherbst, Department of Neuroradiology, University Hospital Heidelberg, 69120 Heidelberg, Germany; dominik.vollherbst@med.uni-heidelberg.de

Received 24 March 2022
Accepted 22 April 2022
Published Online First 4 May 2022

To cite: Schmitt N, Wucherpfennig L, Hohenstatt S, *et al*. *J NeuroIntervent Surg* 2023;**15**:594–599.

ABSTRACT

Background Endovascular embolization using liquid embolic agents (LEAs) is frequently applied for the treatment of intracranial vascular malformations. Appropriate visibility of LEAs during embolization is essential for visual control and to prevent complications. Since LEAs contain different radiopaque components of varying concentrations, our aim was the systematic assessment of the visibility of the most used LEAs in fluoroscopy.

Methods A specifically designed in vitro model, resembling cerebral vessels, was embolized with Onyx 18, Squid 18, Squid 12, PHIL (precipitating hydrophobic injectable liquid) 25%, PHIL LV (low viscosity) and NBCA (n-butyl cyanoacrylate) mixed with iodized oil (n=3 for each LEA), as well as with contrast medium and saline, both serving as a reference. Fluoroscopic image acquisition was performed in accordance with clinical routine settings. Visibility was graded quantitatively (contrast to noise ratio, CNR) and qualitatively (five-point scale).

Results Overall, all LEAs provided at least acceptable visibility in this in vitro model. Onyx and Squid as well as NBCA mixed with iodized oil were best visible at a comparable level and superior to the formulations of PHIL, which did not differ in quantitative and qualitative analyses (eg, Onyx 18 vs PHIL 25% along the 2.0 mm sector: mean CNR±SD: 3.02±0.42 vs 1.92±0.35; mean score±SD: 5.00±0.00 vs 3.75±0.45; p≤0.001, respectively).

Conclusion In this systematic in vitro study, relevant differences in the fluoroscopic visibility of LEAs in neurointerventional embolization procedures were demonstrated, while all investigated LEAs provided acceptable visibility in our in vitro model.

Key messages

⇒ Endovascular embolization of cerebral vascular malformations using liquid embolic agents (LEAs) is a safe and frequently applied treatment mode. Since visibility of these LEAs is essential for visual control and to prevent complications, the aim of the present study was the systematic assessment of the visibility of the most commonly used LEAs in fluoroscopy.

⇒ All investigated LEAs (Onyx 18, Squid 18, Squid 12, PHIL 25%, PHIL LV, NBCA mixed with iodized oil) provided at least acceptable visibility in our in vitro model, while the tantalum-based LEAs Onyx 18, Squid 18, and Squid 12 as well as the embolic agent NBCA mixed with iodized oil provided the best visibility.

⇒ Sufficient visibility of LEAs during embolization and the knowledge of the differences between the agents is mandatory for safe embolization procedures in clinical practice.

INTRODUCTION

Endovascular embolization of cerebral arteriovenous malformations (AVMs) and dural arteriovenous fistulas (dAVFs) using liquid embolic agents (LEAs) is an increasingly applied treatment mode.[1–5] In recent years, several LEAs, each with different properties, became commercially available. The most used copolymer-based, non-adhesive LEAs are Onyx (Medtronic Neurovascular, Irvine, CA), Squid (Balt, Montmorency, France) and the precipitating hydrophobic injectable liquid (PHIL; MicroVention, Aliso Viejo, CA). While Onyx and Squid both consist of ethylene-vinyl alcohol copolymer (EVOH), dimethylsulfoxide (DMSO), and tantalum powder as its radiopaque component, PHIL is based on two specific copolymers, poly(lactide-co-glycolide) and polyhydroxyethylmethacrylate, as its active ingredients and covalently bound triiodophenol enabling intrinsic radiopacity. The major difference between the EVOH-based LEAs Onyx and Squid is the size of the grains of the admixed tantalum powder, which is smaller ('micronized') for Squid, aiming to enhance the homogeneity in radiopacity and thus enabling a better visibility during longer injection times. While Onyx only features the formulation Onyx 18 as its low-viscosity version, the LEAs Squid and PHIL both feature the standard low-viscosity formulations Squid 18 and PHIL 25%, and the extra low-viscosity formulations Squid 12 and PHIL low viscosity (LV). Besides these non-adhesive agents, cyanoacrylates, with its active component n-butyl cyanoacrylate (NBCA), are still applied frequently in several special situations such as for liquid embolization of high-flow shunts in AVMs or dAVFs, for embolization of lesions which cannot be reached with DMSO-compatible catheters, as well as for the pressure-cooker technique.[6 7] NBCA and its derivates are normally mixed with iodized oil to enable a sufficient visibility during endovascular treatment.[6]

Recent publications focused on the imaging artifacts induced by these LEAs in CT and cone beam CT (CBCT).[8–14] However, there are no systematic

studies available investigating the visibility of LEAs in fluoroscopic imaging. Reliable and sufficient visibility of the LEAs during the embolization procedure is essential for visual control regarding the embolized parts of the vascular malformation as well as to prevent possible complications, such as inadvertent embolization of vessels supplying healthy brain or early embolization of the veins of an AVM.

For this reason, the aim of the present study was the systematic assessment of the visibility of the most commonly used LEAs in fluoroscopy using a specifically designed in vitro model.

MATERIALS AND METHODS

Preparation of the in vitro model

For the present study, a novel in vitro model, consisting of the biocompatible synthetic material VisiJet, was specifically designed using a three-dimensional printer. Each model with rectangular shape had a length of 100 mm, a width of 30 mm and a height of 5 mm. At the center of each in vitro model there were merging cylindric shaped cavities with different diameters (21 mm, 20 mm, 1.5 mm, 1.0 mm, and 0.5 mm), resembling cerebral vessels, while the cavity was open to each side.[15] The cylindric cavities with a diameter of 20 mm, 1.5 mm and 1.0 mm had a length of 20 mm each, serving for quantitative and qualitative analysis. The proximal and distal cylindric cavities served for the placement of a 5 French sheath introducer (cavity with diameter of 21 mm, length 10 mm) and to create a continuity of the model to enable complete embolization of the cavities as well as to verify the success of the procedure (cavity with diameter of 0.5 mm, length 30 mm). After the placement of a 5 French sheath introducer, each model (n=3 per LEA, contrast medium and saline) was embolized using a standard embolization microcatheter (SONIC 1.2F; 35 mm detachable tip length; Balt, Montmorency, France) by manual pulsatile LEA injection, using 1 mL DMSO-compatible syringes. Therefore, all LEAs were prepared in accordance with the manufacturer's instructions and as recommended for clinical use. Embolization was conducted for the following LEAs: Onyx 18, Squid 18, Squid 12, PHIL 25%, PHIL LV, NBCA mixed with iodized oil (ratio 1:1; Lipiodol Ultra-Fluid, Guerbet GmbH, Sulzbach/Taunus, Germany) as well as contrast medium (Imeron 300, Bracco Imaging Deutschland GmbH, Konstanz, Germany) and saline (NaCl 0.9%). During the embolization procedure, there was a continuous saline (NaCl 0.9%) flush of 60 mL per hour. Embolization was considered successful when the LEA reached the most distal sector with the smallest diameter (0.5 mm).

A schematic description of the experimental in vitro model is provided in figure 1.

Imaging

Fluoroscopic imaging was performed with standard settings according to clinical routine using the angiography system ARTIS icono (Siemens Heathineers, Erlangen, Germany). A pulsed imaging mode with a pulse rate of 7.5 p/s was used while the store monitor function of the angiography suite was used for image acquisition. The field of view of the receptor was 23 cm. Further imaging settings such as tube parameters, source-image distance (SID) and collimation settings were adjusted automatically by the image quality system OPTICQ (Siemens Healthineers, Erlangen, Germany). To ensure a complete embolization of the in vitro models, each embolization procedure was performed under fluoroscopic guidance.

Quantitative image analysis

Quantitative image analysis of the visibility of the different LEAs and the control groups was conducted on a picture archiving and communication workstation (CENTRICITY PACS 4.0; GE Healthcare, Barrington, IL). Overall, five similar regions of interest (ROI), each rectangular shaped with a length of 4 mm and a width similar to the diameter of each cylindric cavity (2.0 mm, 1.5 mm, and 1.5 mm, respectively), were drawn manually along each sector of the in vitro models and the mean density units (DU) were calculated. Moreover, five square-shaped ROIs, each with a side length of 4 mm, were drawn in proximity on similar levels on the non-cavity part of each in vitro model and the mean background DUs as well as the corresponding standard deviation (SD) were calculated. Each manual drawing was performed in consensus with a neuroradiology resident and a neuroradiology attending (6 years and 9 years of experience in diagnostic imaging, respectively). Since there was no movement during image acquisition, one single frame per embolized in vitro model was analyzed. In a next step the contrast to noise ratio (CNR) of each level was determined using the following formula:[16]

$$CNR = \frac{|\text{Mean DU}_{LEA} - \text{Mean DU}_{background}|}{\text{SD}_{background}}$$

A schematic illustration of the quantitative analysis is provided in figure 1.

Qualitative image analysis

Qualitative analysis of the fluoroscopic images was performed by two different readers (reader 1 and reader 2, both with 6 years of experience in diagnostic imaging) on a picture archiving and communication workstation (CENTRICITY PACS 4.0). To improve the quality of the qualitative analysis, a second read was performed after 3 months. For both reads, each reader was blinded to the type of LEA, contrast medium and saline. Since there is no standard imaging window available for fluoroscopic images, the window settings were left as predetermined by the angiography suite and the PACS workstation with a window width (W) of 4095 DU and a level (L) of 2047 DU. The observers were not allowed to adjust the window settings. The visibility of the embolic agent along each sector (diameter of 2.0 mm, 1.5 mm, and 1.0 mm, respectively) was graded by a five-point scale: (1) no visibility, (2) poor visibility, (3) acceptable visibility, (4) good visibility, and (5) excellent visibility.

Statistics

Statistical analysis was performed using the GraphPad Prism software (version 9.3.1, San Diego, CA). The assessment of the inter-reader and intra-reader agreement for qualitative image analysis was conducted using the Cohen's κ coefficient. The κ values were interpreted as follows: ≤0.20, poor agreement; 0.21–0.40, fair agreement; 0.41–0.60, moderate agreement; 0.61–0.80, good agreement; and 0.81–1.00, very good agreement.[17 18] To evaluate statistical differences between the study groups, the Kruskal-Wallis test was performed. The Dunn's test for multiple comparisons using statistical hypothesis testing was conducted as a pos-hoc test to evaluate differences among the individual LEAs. In order to reduce the number of statistical tests, and thus to reduce the risk of bias by multiple testing, the Dunn's test was only performed for the low-viscosity formulations (Onyx 18 vs Squid 18 vs PHIL 25%), the extra-low-viscosity formulations (Squid 12 vs PHIL LV), and the different versions of Squid (Squid 18 vs Squid 12) and PHIL (PHIL 25% vs PHIL LV). NBCA was compared with all applied LEAs (Onyx

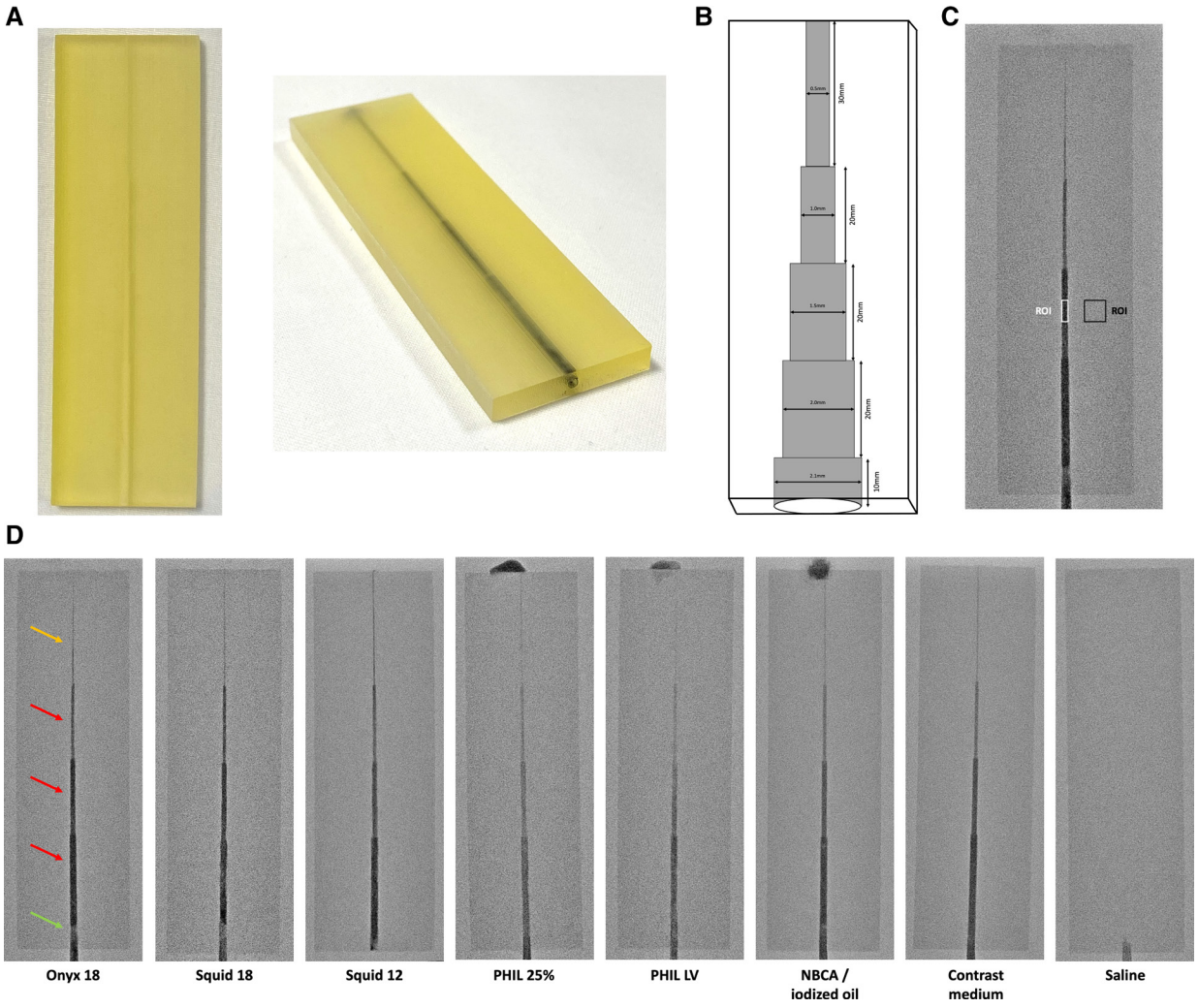

Figure 1 Images of a clean and one Onyx 18 embolized in vitro model (A) as well as a schematic illustration of its structure (B). The image on the right of the upper row (C) illustrates one Onyx embolized in vitro model in fluoroscopy and an exemplary placement of the applied regions of interest (ROI; white: ROI along the 1.5 mm sector; black: ROI drawn on the similar level on the non-cavity part of the in vitro model). Representative fluoroscopic images of the in vitro models embolized with different liquid embolic agents as well as contrast medium and saline, both serving a reference standard, are demonstrated in the lower row (D). The window width was set at 4095 density units (DU) and the window level at 2047 DU. Please note the radiopaque material at the upper end of the different PHIL formulations and NBCA/iodized oil embolized models which is of artificial character and had no influence on the present results. Yellow arrow: sector with a diameter of 0.5 mm to verify the success of the embolization procedure; red arrows: sectors of interest for quantitative and qualitative analysis with a diameter of 2.0 mm, 1.5 mm, and 1.0 mm; green arrow: sector with a diameter of 21 mm for placement of a 5 French sheath introducer. Please note the used microcatheter in the saline filled in vitro model. LV, low viscosity; NBCA, n-butyl cyanoacrylate; PHIL, precipitating hydrophobic injectable liquid.

18, Squid 18, Squid 12, PHIL 25%, and PHIL LV). There was no statistical testing between the LEAs and the control groups (contrast medium and saline) since they only served as a reference standard.

Data of the quantitative analysis are presented as mean CNR±SD and of the qualitative analysis as the mean score±SD. The level of statistical significance was defined as $p<0.05$.

RESULTS

Illustrations of fluoroscopic images of the embolized in vitro models are demonstrated in figure 1. The results of the quantitative image analysis are summarized in figure 2 and table 1. The Kruskal-Wallis test showed a difference among the quantitative visibility of the LEAs along the different sized cylindric cavities (2.0 mm, 1.5 mm, 1.0 mm; $p<0.001$, respectively). Regarding the low-viscosity and extra-low-viscosity formulations of the investigated LEAs, the Dunn's test demonstrated a better visibility of the tantalum-based LEAs Onyx 18, Squid 18 and Squid 12 compared with the triiodophenol-containing LEAs PHIL 25% and PHIL LV (for example, Onyx 18 vs PHIL 25% along all investigated diameters: $p<0.001$, respectively; mean CNR±SD, 2.0 mm: 3.02±0.42 vs 1.92±0.35; 1.5 mm: 2.65±0.32 vs 1.35±0.28; 1.0 mm: 1.76±0.51 vs 0.81±0.13). Further difference was demonstrated between Squid 18 and NBCA mixed with iodized oil along the 2.0 mm sector ($p=0.035$), between Squid 18 and PHIL 25% along the 1.0 mm sector ($p=0.012$) as well as for NBCA mixed with iodized oil and both PHIL formulations, excepting PHIL 25% along the 1.0 mm sector ($p=0.127$).

The results of the qualitative analysis of the fluoroscopic images are summarized in figure 2 and table 2. The inter-reader reliability showed a good agreement ($\kappa=0.757$; range 0.668–0.846), while the intra-reader reliability demonstrated a very good agreement ($\kappa=0.8682$; range 0.800–0.937) for the qualitative analyses by both readers. Dunn's test of the qualitative

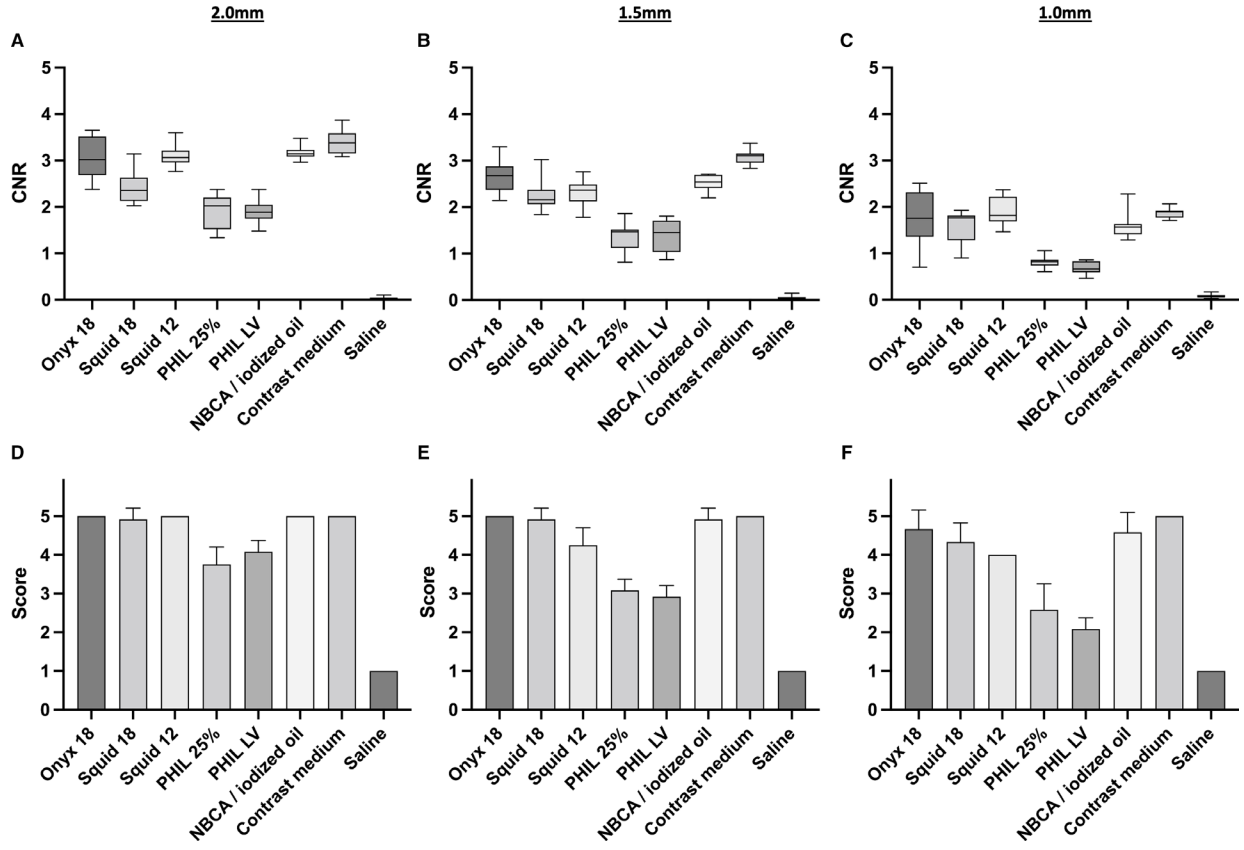

Figure 2 Illustration of the results of the quantitative (A–C) and qualitative (D–F) image analysis for the different sized sectors along the cylindric cavities (2.0 mm, 1.5 mm, 1.0 mm) of the in vitro models. The tantalum containing LEAs Onyx 18, Squid 18, Squid 12 and NBCA mixed with iodized oil (ratio 1:1) were better visible compared with the triiodophenol containing LEAs PHIL 25% and PHIL LV, reaching in most cases statistical significance. Detailed information on the p values are provided in tables 1 and 2. Saline was not visible in both analyses while contrast medium was similar to the tantalum-based LEAs as well as NBCA mixed with iodized oil. Upper row: quantitative analysis, lower row: qualitative analysis; bars: mean; whiskers: SD; diameter 2.0 mm (A, D); diameter 1.5 mm (B, E); diameter 1.0 mm (C, F). CNR, contrast to noise ratio; LEAs, liquid embolic agents; LV, low viscosity; NBCA, n-butyl cyanoacrylate; PHIL, precipitating hydrophobic injectable liquid.

Table 1 Summary of the results of the quantitative analysis

Liquid embolic agent	Onyx 18	Squid 18	Squid 12	PHIL 25%	PHIL LV
Diameter	2.0 mm				
NBCA/iodized oil	p>0.999	**p=0.035**	p>0.999	**p<0.001**	**p<0.001**
PHIL LV	N/A	N/A	**p<0.001**	p>0.999	
PHIL 25%	**p=0.002**	p>0.999	N/A		
Squid 18	p=0.379	N/A	p=0.200		
Diameter	1.5 mm				
NBCA/iodized oil	p>0.999	p>0.999	p>0.999	**p<0.001**	**p<0.001**
PHIL LV	N/A	N/A	**p=0.027**	p>0.999	
PHIL 25%	**p<0.001**	p=0.073	N/A		
Squid 18	p=0.790	N/A	p>0.999		
Diameter	1.0 mm				
NBCA/iodized oil	p>0.999	p>0.999	p=0.520	p=0.127	**p=0.017**
PHIL LV	N/A	N/A	**p<0.001**	p>0.999	
PHIL 25%	**p=0.002**	**p=0.012**	N/A		
Squid 18	p>0.999	N/A	p>0.999		

Bold type indicates statistical significance.
N/A: no p value available since the Dunn's test was only performed for corresponding LEA variants.
LEA, liquid embolic agent; LV, low viscocity; NBCA, n-butyl cyanoacrylate; PHIL, precipitating hydrophobic injectable liquid.

scores demonstrated similar findings compared with the quantitative results. There was a better visibility of the tantalum-based LEAs Onyx 18, Squid 18 and Squid 12 compared with the triiodophenol-based LEAs PHIL 25% and PHIL LV regarding the groups of the low-viscosity and extra-low-viscosity formulations (for example Onyx 18 vs PHIL 25% along all investigated diameters: $p \leq 0.001$, respectively; mean score±SD, 2.0 mm: 5.00±0.00 vs 3.75±0.45; 1.5 mm: 5.00±0.00 vs 3.08±0.289; 1.0 mm: 4.67±0.49 vs 2.58±0.67). All LEAs, including the two formulations of PHIL, provided at least 'acceptable visibility' in qualitative analysis along most sectors of the in vitro models. Statistical difference was not reached between Squid 12 and PHIL LV along the 1.0 mm (p=0.101) and 1.5 mm (p=0.162) sectors. Moreover, there was a better visibility of NBCA mixed with iodized oil compared with both PHIL formulations, while there was no difference compared with the tantalum-based LEAs along all sectors, respectively.

Further details of the results of the quantitative and qualitative analyses are provided in the online supplemental appendix.

DISCUSSION

Endovascular embolization of cerebral AVMs and dAVFs using LEAs is a safe and effective treatment option which has been increasingly applied in the last few years.[1–5] Different embolic agents, each with specific properties, were introduced for this purpose over time.[6] Fluoroscopy is the primary imaging mode

Table 2 Summary of the results of the qualitative analysis by two different readers

Liquid embolic agent	Onyx 18	Squid 18	Squid 12	PHIL 25%	PHIL LV
Diameter	2.0 mm				
NBCA/iodized oil	p>0.999	p>0.999	p>0.999	**p<0.001**	**p=0.002**
PHIL LV	N/A	N/A	**p=0.002**	p>0.999	
PHIL 25%	**p<0.001**	**p<0.001**	N/A		
Squid 18	p>0.999	N/A	p>0.999		
Diameter	1.5 mm				
NBCA/iodized oil	p>0.999	p>0.999	p=0.579	**p<0.001**	**p<0.001**
PHIL LV	N/A	N/A	p=0.162	p>0.999	
PHIL 25%	**p<0.001**	**p<0.001**	N/A		
Squid 18	p>0.999	N/A	p=0.579		
Diameter	1.0 mm				
NBCA/iodized oil	p>0.999	p>0.999	p>0.999	**p=0.003**	**p<0.001**
PHIL LV	N/A	N/A	p=0.101	p>0.999	
PHIL 25%	**p=0.001**	**p=0.034**	N/A		
Squid 18	p>0.999	N/A	p>0.999		

Bold type indicates statistical significance.
N/A: no p value available since the Dunn's test was only performed for corresponding LEA variants.
LEA, liquid embolic agent; LV, low viscosity; NBCA, n-butyl cyanoacrylate; PHIL, precipitating hydrophobic injectable liquid.

for visualization of LEAs during these treatments. However, there are currently no studies available investigating the fluoroscopic visibility of LEAs. In the present study we performed a systematic in vitro analysis of the clinically most used LEAs and demonstrated that these LEAs significantly differ in visibility. The tantalum-containing LEAs Onyx 18, Squid 18, Squid 12 as well as NBCA mixed with iodized oil (ratio 1:1) provided the best visibility. Nevertheless, all investigated LEAs, including both formulations of PHIL, which use triiodophenol for visibility, provided acceptable visibility along most cavities in this in vitro study.

In recent years, several studies investigated the degree of LEA-induced imaging artifacts in CT and CBCT as well as options for artifact reduction, whereas no study focused on the fluoroscopic visibility of LEAs until now, which is an essential feature of LEAs to enable visual control of the distribution of the embolic agent during the embolization procedure.[8 10–14] These artifact-investigating studies demonstrated that the tantalum containing LEAs, such as the different formulations of Onyx and Squid, induce more artifacts compared with the embolic agents containing iodine as its radiopaque component, for example, the formulations of PHIL or NBCA mixed with iodized oil.[8 10 11] The present study revealed similar findings, with a better visibility of the tantalum-based LEAs Onyx and Squid. Similar to the artifacts, a possible reason is the higher atomic number of the admixed tantalum (atomic number 73) compared with iodine (atomic number 53) as part of the different PHIL formulations. The higher the atomic number of a material, the higher its density, leading to a higher absorption of x-rays, finally resulting in a better visibility of the LEA in fluoroscopy.

Moreover, a further impact on the visibility can be attributed to the amount of the admixed radiopaque component. Since the embolic agents NBCA/iodized oil and the formulations of PHIL both include iodine as its radiopaque component, the higher amount of iodine within the ratio of 1:1 for NBCA mixed with iodized oil probably causes its better visibility.

In a few comparisons, we did not observe the expected differences between the tantalum-based LEAs and the iodine-based materials. For example, there was a quantitatively better visibility of Squid 12 compared with PHIL LV along the 2.0 mm sector (p=0.002), while statistical difference was not reached along the 1.5 mm (p=0.162) and 1.0 mm (p=0.101) sectors. A possible reason for these findings might be an inhomogeneous dilution of the LEA with saline within individual sectors of the in vitro model while having a continuous saline flush during the embolization procedure.

Since there are no comparable studies available investigating the fluoroscopic visibility of LEAs, one strength of the present study is the usage of a novel, specifically designed, in vitro model with different sized cylindric cavities, resembling cerebral vessels of various calibers, and thus enabling a standardized and reproducible comparison of the individual embolic agents. Further investigation of contrast medium and saline was performed, both serving as a reference. Moreover, embolization was conducted in accordance with the clinical treatment routine, and quantitative as well as qualitative analysis of all commonly used LEAs was performed by two experienced readers.

Besides fluoroscopic imaging, roadmap-based imaging techniques are commonly used for embolization of vascular malformations in clinical practice. However, we consciously did not focus on roadmap-based imaging since this technique is based on post-processing of fluoroscopic images. Therefore, focusing on the fluoroscopic images has the potential to avoid additional influence by computational post-processing and enables the analysis of the pure visibility of the embolic agents.

An advantage of our study is that we used a standardized in vitro model. However, in clinical practice, the visibility of the LEA can be impaired by bony structures, the LEA cast, or other foreign materials. In our study, all LEAs featured at least 'acceptable visibility' across most of the cavities of the model. During embolization in clinical practice, this 'acceptable visibility' might be insufficient in special situations with small vessels and superimposing structures. However, in the published clinical studies, including the clinical and experimental studies which were published on PHIL, all of the examined agents were described to be adequately visible.[19–22]

We acknowledge that this study has several limitations. In general, the transferability of an in vitro model to clinical treatment of humans is limited since the properties of the LEAs relate to the physical properties of blood, such as the pH value, electrolyte concentration, or temperature. Moreover, only a number of three samples per LEA was investigated due to the intense costs of the novel in vitro models and the used LEAs. However, the findings were consistent across the study groups. Only one mixture of NBCA mixed with iodized oil (ratio 1:1) was investigated while different concentrations may result in different findings. Since our in vitro model features the advantage of being not water-soluble, the used material as well as its design have only limited similarity to the density of the human skull. Furthermore, the imaging setting and especially the kilovoltage potential (kVp) were set automatically by the OPTICQ (Siemens Healthineers, Erlangen, Germany) imaging mode of the angiography system with no option for manual adjustment. Therefore, the applied kVps were about a third lower compared with clinical settings which might cause a different CNR at clinical levels.

CONCLUSION

In this study, a systematic analysis of the fluoroscopic visibility of the most commonly used LEAs was performed, using a novel in vitro model. There was a statistical difference between all

investigated LEAs, while the tantalum-based LEAs Onyx 18, Squid 18, and Squid 12 as well as the embolic agent NBCA mixed with iodized oil (ratio 1:1) provided the best visibility. However, all investigated LEAs, including both formulations of PHIL, which use triiodophenol for visibility, provided acceptable visibility along most sections of our in vitro model.

Contributors NS, MB, MAM and DFV initiated the project. NS and DFV led the research, conducted the data acquisition, statistical analysis and wrote the manuscript. MB, MAM and DFV were involved in the study design and concept. DFV is the guarantor of this work. LW, SH, CSW and CMS participated in data acquisition. All authors discussed the results, commented on the paper, and approved the final version of the manuscript.

Funding The authors have not declared a specific grant for this research from any funding agency in the public, commercial or not-for-profit sectors.

Competing interests None declared.

Patient consent for publication Not applicable.

Ethics approval Not applicable.

Provenance and peer review Not commissioned; externally peer reviewed.

Data availability statement All data relevant to the study are included in the article or uploaded as supplementary information. All relevant data generated or analyzed during this study are included in this published article (and its supplementary information files).

ORCID iDs
Niclas Schmitt http://orcid.org/0000-0003-2509-5459
Lena Wucherpfennig http://orcid.org/0000-0002-2280-1269
Sophia Hohenstatt http://orcid.org/0000-0003-0951-3948
Charlotte S Weyland http://orcid.org/0000-0002-1374-7854
Dominik F Vollherbst http://orcid.org/0000-0002-8992-4757

REFERENCES

1 Gross BA, Du R. Diagnosis and treatment of vascular malformations of the brain. *Curr Treat Options Neurol* 2014;16:279.
2 Friedlander RM. Clinical practice. Arteriovenous malformations of the brain. *N Engl J Med* 2007;356:2704–12.
3 Chen C-J, Ding D, Derdeyn CP, *et al*. Brain arteriovenous malformations: a review of natural history, pathobiology, and interventions. *Neurology* 2020;95:917-927.
4 Wu EM, El Ahmadieh TY, McDougall CM, *et al*. Embolization of brain arteriovenous malformations with intent to cure: a systematic review. *J Neurosurg* 2019;132:388–99.
5 Gross BA, Albuquerque FC, Moon K, *et al*. Evolution of treatment and a detailed analysis of occlusion, recurrence, and clinical outcomes in an endovascular library of 260 dural arteriovenous fistulas. *J Neurosurg* 2017;126:1884–93.
6 Vollherbst DF, Chapot R, Bendszus M, *et al*. Glue, Onyx, Squid or PHIL? Liquid embolic agents for the embolization of cerebral arteriovenous malformations and dural arteriovenous fistulas. *Clin Neuroradiol* 2022;32:25–38. doi:10.1007/s00062-021-01066-6
7 Chapot R, Stracke P, Velasco A, *et al*. The pressure cooker technique for the treatment of brain AVMs. *J Neuroradiol* 2014;41:87–91.
8 Schmitt N, Floca RO, Paech D, *et al*. Imaging artifacts of nonadhesive liquid embolic agents in conventional and cone-beam CT in a novel in vitro AVM model. *Clin Neuroradiol* 2021;31:1141–8. doi:10.1007/s00062-021-01013-5
9 Otsuka T, Nishihori M, Izumi T, *et al*. Streak metal artifact reduction technique in cone beam computed tomography images after endovascular neurosurgery. *Neurol Med Chir* 2021;61:468–74.
10 Schmitt N, Floca RO, Paech D, *et al*. Imaging artifacts of liquid embolic agents on conventional CT in an experimental in vitro model. *AJNR Am J Neuroradiol* 2021;42:126-131.
11 Pop R, Mertz L, Ilyes A, *et al*. Beam hardening artifacts of liquid embolic agents: comparison between Squid and Onyx. *J Neurointerv Surg* 2019;11:706–9.
12 Vollherbst DF, Otto R, Do T, *et al*. Imaging artifacts of Onyx and PHIL on conventional CT, cone-beam CT and MRI in an animal model. *Interv Neuroradiol* 2018;24:693–701.
13 Schmitt N, Weyland CS, Wucherpfennig L, *et al*. The impact of software-based metal Artifact reduction on the liquid Embolic agent Onyx in cone-beam CT: a systematic in vitro and in vivo study. *J Neurointerv Surg* 2022;14:832–6.
14 Schmitt N, Weyland CS, Wucherpfennig L, *et al*. Iterative metal artifact reduction (iMAR) of the non-adhesive liquid embolic agent Onyx in computed tomography: an experimental study. *Clin Neuroradiol* 2021. doi:10.1007/s00062-021-01101-6. [Epub ahead of print: 13 Oct 2021].
15 Saeki N, Rhoton AL. Microsurgical anatomy of the upper basilar artery and the posterior circle of Willis. *J Neurosurg* 1977;46:563–78.
16 Goode AR, Snyder C, Snyder A, *et al*. Signal and contrast to noise ratio evaluation of fluoroscopic loops for interventional fluoroscope quality control. *J Appl Clin Med Phys* 2019;20:172–80.
17 Altman DG. *Practical statistics for medical research*. CRC press, 1990.
18 Cohen J. A coefficient of agreement for nominal scales. *Educ Psychol Meas* 1960;20:37–46.
19 Vollherbst DF, Otto R, von Deimling A, *et al*. Evaluation of a novel liquid embolic agent (precipitating hydrophobic injectable liquid (PHIL)) in an animal endovascular embolization model. *J Neurointerv Surg* 2018;10:268–74.
20 Vollherbst DF, Otto R, Hantz M, *et al*. Investigation of a new version of the liquid embolic agent PHIL with extra-low-viscosity in an endovascular embolization model. *AJNR Am J Neuroradiol* 2018;39:1696–702.
21 Lamin S, Chew HS, Chavda S, *et al*. Embolization of intracranial dural arteriovenous fistulas using PHIL liquid embolic agent in 26 patients: a multicenter study. *AJNR Am J Neuroradiol* 2017;38:127–31.
22 Samaniego EA, Kalousek V, Abdo G, *et al*. Preliminary experience with precipitating hydrophobic injectable liquid (PHIL) in treating cerebral AVMs. *J Neurointerv Surg* 2016;8:1253–5.